Procedia Manufacturing

Volume 1, 2015, Pages 728–739

43rd Proceedings of the North American Manufacturing Research Institution of SME http://www.sme.org/namrc

Finite Element Simulation and Validation of Chip Formation and Cutting Forces in Dry and Cryogenic Cutting of Ti–6Al–4V

A. Davoudinejad[1*],E. Chiappini[2], S. Tirelli[2], M. Annoni[1] and M. Strano[1]

[1]*MechanicalEngineeringDepartment, Politecnico di Milano, via La Masa 1, 20156 Milano, Italy*

[2]*LaboratorioMUSP,viaTirotti9,29122Piacenza,Italy.*

**ali.davoudinejad@polimi.it*

Abstract

Ti-6Al-4V titanium alloy is a popular material in industrial applications (e.g. aerospace, oil & gas, medical) due to its superior mechanical properties, although its low thermal conductivity and high chemical reactivity with other materials make it a hard-to-cut material. A finite element model (FEM) was developed in the present investigation to simulate dry and cryogenic orthogonal cutting of Ti-6Al-4V by using TiAlN coated carbide inserts. Numerical prediction of the effect of the superior cryogenic cooling on chip formation, cutting and thrust forces were investigated. The simulations were validated by the comparison with experimental results. The model calibration was performed with experimental data on dry cutting and then the model was used for predicting the cryogenic cooling case. The validated FEM models were used to compare the chip formation in dry cutting and cryogenic cutting in order to point out some differences in terms of chip segmentation frequency and chip thickness and gain additional knowledge.

Keywords: Cryogenic machining, Titanium machining, Finite element modeling, Cutting forces, Chip formation.

1 Introduction

Superior properties of titanium alloy Ti-6Al-4V (Grade 5 titanium) such as high strength to weight ratio, low density, high toughness, excellent corrosion resistance, and bio compatibility make it well suited for a large range of applications and widely adopted in various manufacturing operations. Machinability of Grade 5 titanium is extremely low due to the brittle nature, high chemical reactivity at elevated temperatures, low rigidity and low thermal conductivity of this material, which cause extremely high temperatures at the tool-chip interface (Byrne et al., 2003). Many researchers performed experimental studies to improve the machinability of Grade 5 titanium alloy attempting to decrease manufacturing costs, for example by improving cutting tool materials and coatings (Corduan et al., 2003). An experimental study performed to estimate the tool life and other variables of interest

Peer-review under responsibility of the NAMRI Scientific Committee

doi:10.1016/j.promfg.2015.09.037

with different process parameters. The cutting performance of an innovative TiAlN coating obtained by Physical Vapor Deposition (PVD) magnetron sputtering and the effects of a Deep Cryogenic Treatment (DCT) on the tools were investigated (Strano et al., 2013). Another study regarding machinability was performed by (Ali et al., 2011). The authors performed machining tests with three types of cooling techniques (nitrogen gas, high pressure coolant (HPC) and cryogenic cooling) and made a comparison to investigate a potential increase in machining productivity with innovative cooling methods. Investigations on other machining technologies, such as thermally assisted machining, have been developed to increase machinability (Sun et al., 2010). (Sun et al., 2008) performed laser assisted machining (LAM) and hybrid machining to improve the tool life and the material removal rate. The tool cooling strategy plays a significant role on machining operations to increase tool life: cryogenic cooling has been determined as one of the most promising methods for hard-to-cut materials and numerous researches are recently investigating it (Yildiz and Nalbant, 2008). A number of studies have investigated the use of liquid nitrogen as coolant for titanium turning and comparisons were made with dry and other coolants, pointing out significant improvements (Venugopal et al., 2007) (Bermingham et al., 2011) (Khan and Ahmed, 2008). Considering the high cost and time consumption of the extensive physical experimentations needed to optimize the cutting conditions and to select the most suitable tool material and geometry, modeling and simulation techniques of machining can minimize expensive testing and determine industry relevant outcomes to improve productivity and enhance product quality (Arrazola et al., 2013). The finite elements model results are greatly influenced by the selected input values, for example material constitutive law or friction model. A reliable material model that perfectly captures the constitutive behavior of the alloy under high strain, strain rate and temperature is critical in machining simulation. A numbers of different material models have been reported in the literature such as the Johnson-Cook (J-C) model (Johnson and Cook, 1983), modified JC models (Calamaz et al., 2008), Oxley's constitutive model (Oxley, 1966) and Power law model (Man et al., 2012), in order to more accurately capture the material behavior. Moreover, the frictional conditions between the tool and the workpiece as well as at the tool-chip interface are as important as the flow stress characterization of the work material. Investigations were performed on tool-chip contact friction numerical modeling and applied into the Finite Element Method (Arrazola and Özel, 2010). Friction coefficient is a significantly influential parameter in numerical results: (Özel, 2006) investigated the effect of the tool-chip interfacial friction model on FEM results and reported that more realistic results can be provided by using a variable friction model.

Several studies performed numerical simulation to investigate the effects of machining parameters, tool materials and coatings. Effects of cutting speed, feed and depth of cut were investigated in corner milling on the tool rake face temperature for optimizing cutting conditions (Ma et al., 2014). The effect of single and multi-layer TiAIN and CBN coatings was experimented and the finite element simulation was used to investigate tool temperatures and wear development (Özel et al., 2010). (Pusavec et al., 2014) presented an experimental investigation of Inconel 718 alloy machined by carbide tools when delivering different phases of nitrogen (gas and liquid). A novel optical nitrogen phase sensor was used and a simplified finite element model of cryogenic machining was simulated to observe the machining process behavior with the different coolant phases. Other investigations were focused on the chip formation mechanics of Ti-6Al-4V in turning with sinusoidal spindle speed variation and constant speed machining. The FE model took into account the micro geometry of the insert and the coating (Chiappini et al., 2014). Other researchers experimentally evaluated the machinability of Ti-6Al-4V and compared results with finite element simulations (Pervaiz et al., 2014) (Li and Shih, 2005) (Ali et al., 2013). Very few papers have been found in the scientific literatures that deal with the simulation of cryogenic machining (Pusavec et al., 2014) (Hong and Ding, 2001). Even less publications (Pu et al., 2014) directly address and explain the specific issues involved in this kind of simulation.

With the present paper we aim at contributing in this line of studies, describing what assumptions and modifications can be implemented in order to transform an FEM model developed and validated for traditional machining, into a model that reliably predicts cryogenic machining. A 2D finite element model is first implemented adopting AdvantEdge®FE software, and experimentally validated by using data on cutting forces and chip geometry. Once the traditional model has been verified, the same material constitutive law has been used in the simulation of orthogonal cryogenic turning. The original model has been transformed by using a different (increased) coefficient of friction and different thermal boundary conditions. Again, the results of the cryogenic FEM have been verified by means of experimental tests, in terms of cutting forces and chip morphology, showing very good agreement.

The results of the dry and cryogenic FEM models are finally compared in order to highlight the differences in the mechanics of chip formation, in terms of state of stress, shear angle and chip morphology.

2 Experimental setup and results

Orthogonal turning of Ti-6Al-4V titanium alloy tubes (diameter 42 mm, wall thickness 1.6 mm) has been performed using Sandvik TiAlN coated carbide inserts with ISO designation CNMG 120408 SMR 1115, using a Sandvik PCLNL 2525M tool holder. The experimental setup is illustrated in Fig.1(a). The combination of the selected inserts and tool holder generates a 4.6˚ rake angle and a 5.4˚ clearance angle. All the machining tests were carried out by using a CNC Somab Unimab 400 lathe with a maximum spindle speed of 2560 rev/min and a maximum power of 11kW. The cutting forces were experimentally measured with a Kistler 9265 dynamometer. According to previous experimental investigations on titanium alloys, cutting speeds for Ti-6Al-4V are generally limited to a maximum of 60 m/min (Ezugwu and Wang, 1997). In this paper, two cutting speeds (40 m/min and 50 m/min) and two feed rates (0.2 mm/rev and 0.3 mm/rev) were considered. For the cryogenic machining, the liquid nitrogen jet was applied to the tool simultaneously at the rake face, at the flank and at the secondary cutting edge as shown in Fig. 1(b).

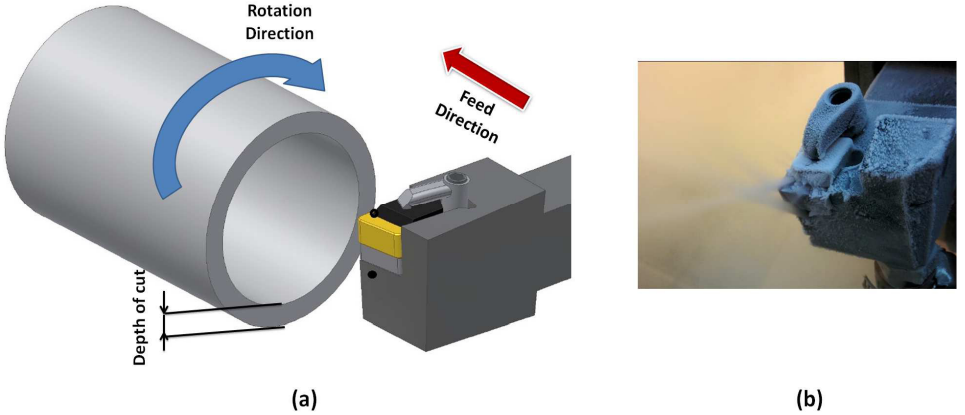

Figure 1: (a) Experimental setup for orthogonal turning (b) tool setup in cryogenic cooling

The liquid nitrogen jets were addressed to the cutting zone with suitable flow rate and pressure. Three replicates were performed for each cutting condition to guarantee statistical consistency. The average force results are presented in Table 1. Images of the chip geometry were captured and measured with an optical digital microscope.

Cutting speed Vc(m/min)	Feed f(mm/rev)	Fc(N)	Ft(N)	μ (Dry)	μ (Cry)
40	0.2	554	265	0.58	0.68
50	0.2	555	268	0.59	0.67
40	0.3	790	329	0.51	0.58
50	0.3	741	308	0.51	0.56

Table 1: Experimental cutting force results

3 Finite element setup

3.1 FE model of dry machining

The predicted results may vary with input data and software so an adequate choice of the software is significant to obtain reliable results (Bil et al., 2004). The special purpose AdvantEdge® FEM software (by Third Wave Systems) specifically for modeling machining processes, was used. The model employs a Lagrangian explicit finite element formulation that can perform coupled thermo-mechanical transient analysis. Fig. 2 shows the setup and the general geometry of the FEM simulation in orthogonal cutting. The workpiece bottom boundary nodes are fixed in *Y* direction and the tool in both *X* and *Y* directions. The rigid cutting tool was meshed using 3070 brick elements.

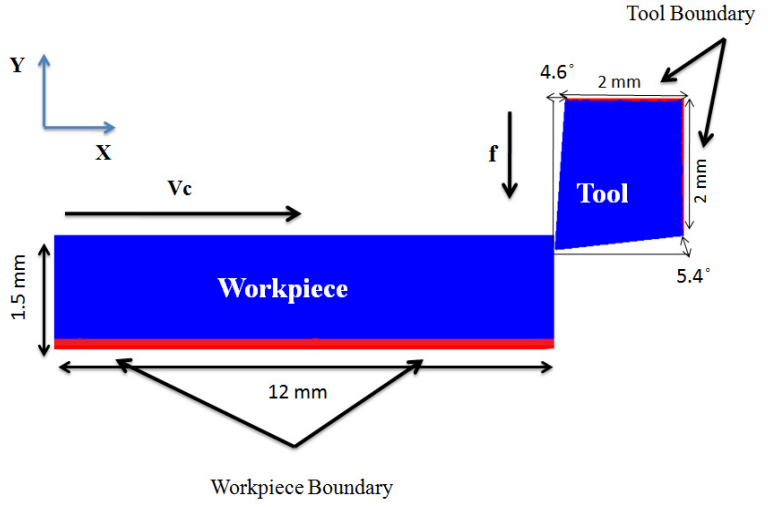

Figure 2: General geometry and setup of the finite element model

The workpiece was meshed with six-node quadratic triangular elements for a total number of 28000 nodes. The maximum and minimum element sizes for the workpiece were set to 0.1 mm and 0.02 mm respectively. The maximum element size of the cutter was set at 0.2 mm and the minimum at 0.02 mm. A high mesh density was defined on the workpiece region near the cutting zone (Fig. 4). Adaptive remeshing is used in order to avoid the inaccuracies due to elemental distortion, inherent to the Lagragian formulation. The mesh quality is constantly monitored during the simulations and when the element distortion reaches a certain tolerance, adaptive remeshing is triggered. In addition to remeshing, refinement and coarsening operators are applied in various parts of the mesh (Man et al., 2012) (Chiappini et al., 2014). The mesh refinement factor was set at the finest value of 8 and coarsening factor was set to 1. The input parameters are summarized in Table 2.

Workpiece		Tool		Process	
Length	12 mm	Rake angle	4.6˚	Cutting speed	40, 50m/min
Height	1.5mm	Clearance angle	5.4˚	Feed	0.2,0.3 mm/rev
Material	Ti-6Al-4V	Cutting edge radius	0.05mm	Depth of cut	1.6 mm
		Material	WC	Length of cut	2 mm
		Coating	TiAlN	Coolant	Cryogenic/Dry

Table 2: Software input parameters

The constitutive model used for flow stress updating is known only in tabular form. It exhibits strain rate hardening, temperature softening, strain hardening in the low strain region and strain softening in the high strain region. A flow stress graph is shown in Fig. 3 where, in order to enhance the graph clarity, only a small subset of the data is plotted.

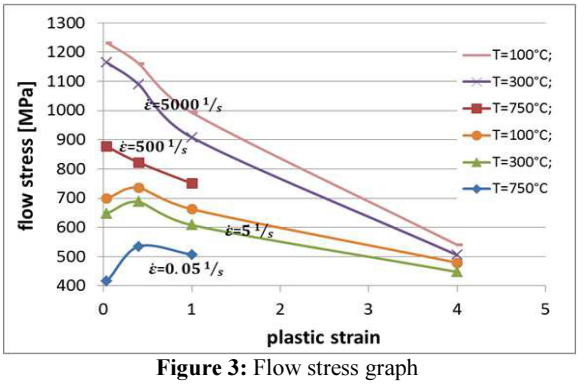

Figure 3: Flow stress graph

The friction phenomenon at the chip-tool interface was modeled using the Coulomb law, as shown in Eq. (1). The frictional stresses τ on the tool rake face are assumed to be proportional to the normal stresses σ_n with a coefficient of friction μ (Arrazola and Özel, 2010).

$$\tau = \mu\sigma_n \tag{1}$$

The mean coefficient of friction between the tool and the chip in orthogonal cutting is generally calculated starting from the experimental measures of cutting forces. In Eq. (2), F_t represents the thrust force, F_c the main cutting force and α is the tool rake angle. Table 1 shows the coefficients of friction calculated with Eq. (2) for different conditions in dry and cryogenic machining. However the average coefficients of friction were used as constant values in simulating different external cooling conditions: 0.55 and 0.62 for dry and cryogenic machining respectively.

$$\mu = \frac{F_t + F_c \tan\alpha}{F_c - F_t \tan\alpha} \tag{2}$$

This approach is in line with our experimental tests, although it is in contrast with some previous results in the literature: Shane et al. found that the cryogenic coolant reduces the temperature at the tool-chip interface but also the coefficient of friction (Hong, Ding and Jeong, 2001).

3.2 FE model of cryogenic machining

In order to simulate the effect of cryogenic cooling, a focused location window where heat exchange by convection takes place is centered around the initial workpiece and moves along with the workpiece. The environmental temperature is set at 20°C, except for a spot (called the jet radius),

which is kept at the liquid nitrogen temperature -190 °C. Both the tool and the work might exchange heat to the environment, within the aforementioned window. They also can exchange heat by internal conduction and at the tool-workpiece interface. It is clear that the two most important parameters for realistically defining the thermal boundary conditions are the jet radius and the surface heat transfer coefficient at the interface. No temperature measurements could be taken in the proximity of the tool tip. However, we do have some temperature measurements and known facts: 1) the temperature of the jet at the rake face impingement location is -170 °C, 2) the workpiece temperature, at its left boundary (Fig. 4) must be practically unchanged during the process, 3) the tool temperature about 1 mm to the right and above the tool tip must be smaller than 300 °C. This last indication comes from a preliminary experimental plan, run with a thermocouple inserted inside a hole drilled din the insert, but the reliability and robustness of this measurements does not allow to indicate a precise number: we were only able to establish an upper bound. Starting with this very rough experimental thermal map, several combinations of jet radius (from 1 to 3 mm) and heat transfer coefficient (46.75 to 5000 kW/(m^{2}K)) were tested. This range has been selected according to the literature review. As an example, a study about cryogenic machining of AZ31B Mg alloy considered local convection coefficient as 5000 kW/(m^{2}K) (Pu et al., 2014). In another research liquid nitrogen was applied to Ti-6Al-4V cutting and finite element simulation estimated the cutting temperature: the average heat transfer was estimated between 23.27 and 46.75 kW/(m^{2}K) (Hong and Ding, 2001). Some example of output FEM thermal maps are shown in Fig. 5 and 6. The combination that is not in contrast with considerations 1), 2) and 3) is obtained when using a jet radius equal to 1.5 mm and a heat transfer coefficient set to 2000 kW/(m^{2}K). This value is overestimated (with respect to reality) but allows the simulation to rapidly reach a steady state for the temperature field. This practice is in line with previous works from different authors.

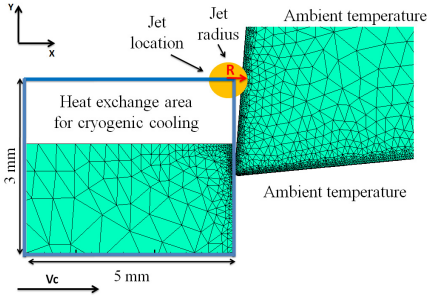

Figure 4: Mesh and heat exchange area for the cryogenic coolant setup

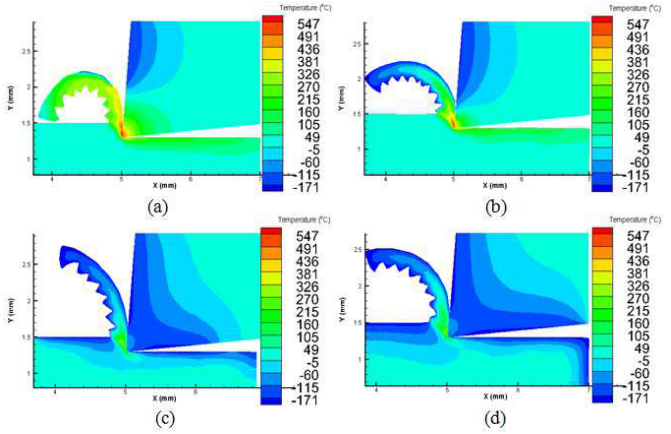

Figure 5: Jet radius (a) 1 mm (b) 1.5 mm (c) 2 mm (d) 3 mm

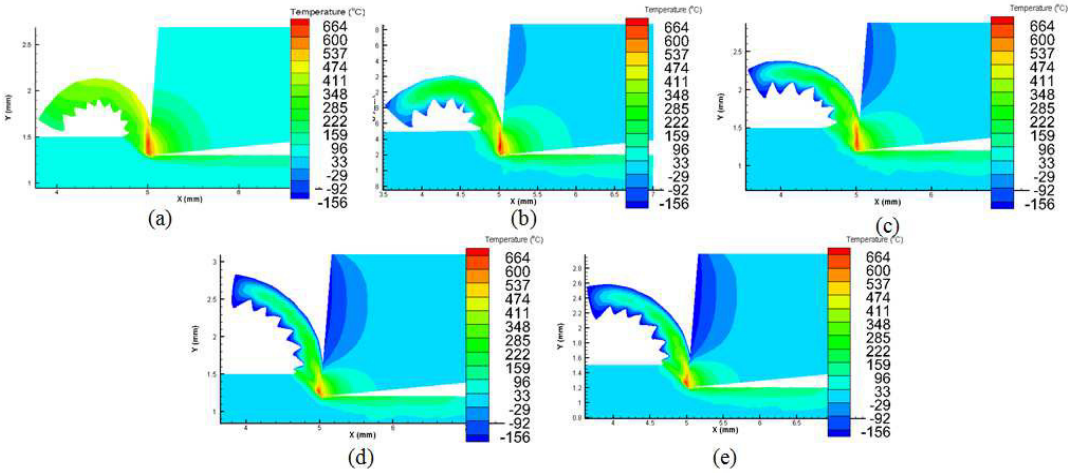

Figure 6: Predicted temperature distribution:(a) h_{cryo}= 46.75 kW/(m^2K) (b) h_{cryo}= 200 kW/(m^2K), (c) h_{cryo}= 500 kW/(m^2K), (d) h_{cryo}= 2000 kW/(m^2K), (e) h_{cryo}= 5000 kW/(m^2K)

4 Validation and discussion of results

4.1 Validation of dry cutting FE model

In this section, a comparison between numerical and experimental results in dry cutting conditions is performed to validate the FE model results. In all the simulations, data were collected after that steady state conditions were reached for both temperature and cutting forces. A comparison was made between experiments and simulated cutting forces, thrust forces and chips. As aforementioned, Ti-6Al-4V mostly generated serrated chip at low cutting speeds (Özel, 2006). Comparison of chip geometry with experiments is shown in Fig. 7 and Table 3. The results indicate close agreement on chip geometry in various cutting conditions. Chip morphology can be described using some parameters such as minimum and maximum values of peak heights, valley heights and peak-peak distances as shown in Fig. 7(a). Temperature prediction is presented in Fig. 7 and shows that increases in cutting speed and feed causes a higher cutting temperature at the tool-chip contact area. The predicted temperature reached a maximum of 770 ℃ localized at the chip-tool contact area. Other researchers reported that the temperature at the cutting zone, at moderate cutting speed, is generally around 900℃ (Venugopal et al., 2007) (Narutaki et al., 1983).

Vc	f		Peak height (μm)		Valley height (μm)		Peak-peak distance (μm)	
			Max	Min	Max	Min	Max	Min
40	0.2	FEM	300	281	228	190	115	101
		Experiment	297	269	186	166	134	121
50	0.2	FEM	297	275	201	167	136	97
		Experiment	285	255	184	157	170	144
40	0.3	FEM	413	393	302	273	210	160
		Experiment	438	414	317	291	163	147
50	0.3	FEM	418	391	276	252	219	178
		Experiment	421	395	278	256	227	179

Table 3: Chip morphology obtained by experiments and FEM in drymachining conditions

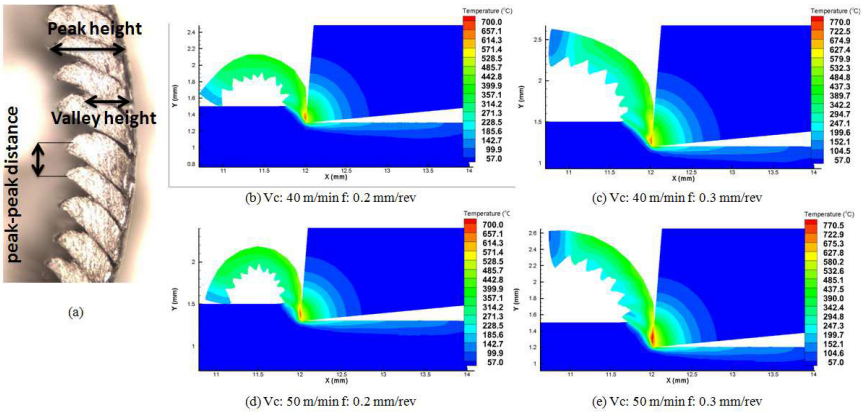

Figure 7: Dry machining: experimental chip at 50 m/min and 0.2 mm/rev (a); simulated serrated chips at various cutting conditions (b) to (e)

A comparison between experimental and simulated cutting and thrust forces under different cutting conditions is shown in Fig. 8. The results indicate that there is a good agreement between experimental and simulated values for main cutting force (approximately 10% error) and thrust force (7% error).

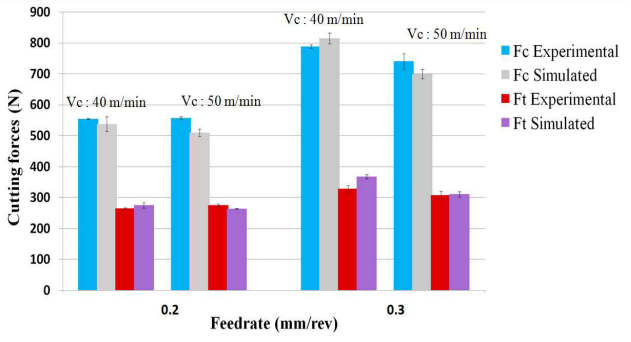

Figure 8: Comparison of measured and simulated forces

4.2 Validation of cryogenic cutting FE model

Numerical simulation of cryogenic cooling was setup based on the dry machining FE model setting with identical cutting conditions. The comparison between experimental and predicted chip morphology is reported in Fig. 9 and in Table 4 and shows a very good agreement between experimental and numerical results concerning the chip geometric parameters (peak height, valley height, peak-peak distance). On the Fig. 9, numerically obtained chips for different cutting speeds and feeds are compared with experiments. The effect of cryogenic cooling can be observed at the cutting tool, chip and workpiece machined surface area: the cryogenic coolant mainly affects the temperature distribution of the formed chip and the tool rake face, where the jet impinged at the machining area. However, the cutting edge, which is not in direct contact with the coolant, presents a much higher temperature, (about 700 ° C) observed at steady state over a narrow area on the tool-chip interface. Different distribution of temperature occurs due to the cutting conditions. The largest temperature dispersion is observed at Vc= 50 m/min and f= 0.2 mm/rev. The cooling effect on the serrated chips is greater at lower feed. Finally, the cutting forces were compared between the simulation and

experimental results in cryogenic machining as shown in Fig. 10. The predicted cutting forces during cryogenic machining conditions present good agreement with experimental results and were higher than those obtained with dry machining. The percent error between experimental and simulated forces is approximately 6% for the main cutting force and 8% for the thrust force. Influence of workpiece temperature plays a significant role on cutting force prediction, i.e. the cutting forces increase because of the strong cooling effect of cryogenic coolant on the workpiece, which makes it harder (Zhao and Hong, 1992).

Vc	f		Peak height (µm)		Valley height (µm)		Peak-peak distance (µm)	
			Max	Min	Max	Min	Max	Min
40	0.2	FEM	274	258	171	157	209	169
		Experiment	313	236	153	129	202	121
50	0.2	FEM	276	246	184	143	186	126
		Experiment	266	205	146	104	165	124
40	0.3	FEM	411	379	263	257	276	177
		Experiment	414	368	245	171	272	139
50	0.3	FEM	405	365	273	246	259	216
		Experiment	417	321	250	170	227	184

Table 4: Chip morphology obtained by experiments and FEM in cryogenic machining conditions

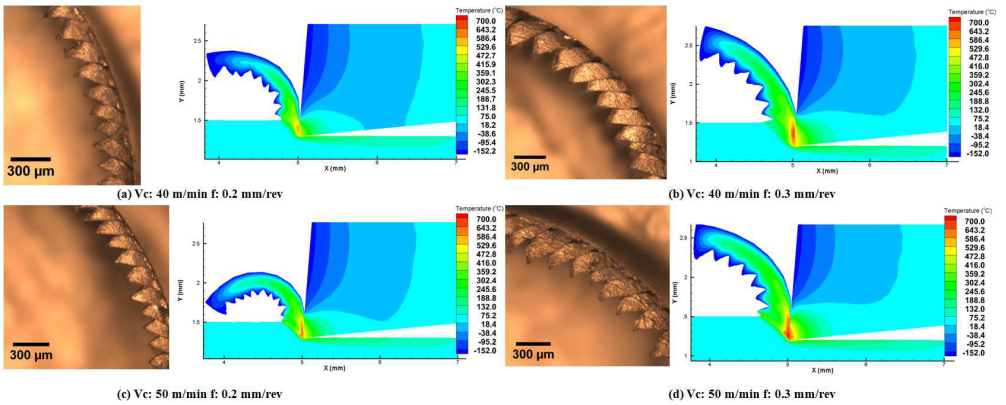

Figure 9: Experimental (left) and simulated (right) serrated chips in various cutting conditions at cryogenic machining

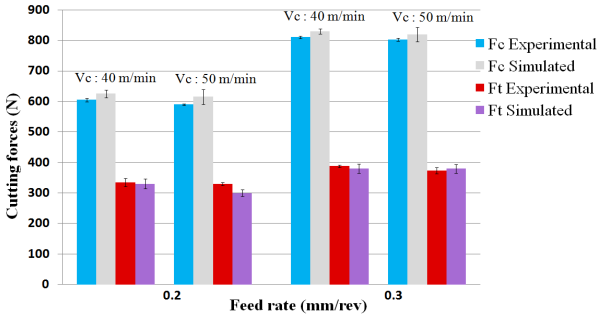

Figure 10: Comparison of measured and simulated forces for cryogenic machining

4.3 Comparison of dry and cryogenic cutting

The validated FEM models allow to compare how the mechanics of material removal changes, at the same cutting conditions, switching from dry to cryogenic machining. It is clear from Table 5 that the segmentation frequency of the chip is significantly reduced (larger peak-peak distance). Valley heights seem to get smaller than peak heights; this could lead to a more corrugated chip internal face, on the way to a possible chip breakage. In other words, it appears that cryogenic cooling increases the duration of the thermal cycle responsible for the aerospace titanium chip segmentation and, in general, reduces the chip thickness. This fact could be related to the increased hardness achieved by the target material. Fig. 11 shows the stress distribution in dry and cryogenic cutting. The stress distributed at slightly larger area of the tool chip contact in cryogenic cutting than dry cutting. Moreover, the workpiece material seems to be more affected by the cutting action upstream the shear plane. This phenomenon seems to be related to the lower segmentation frequency, which creates bigger portion of material between consecutive chip valleys.

		Peak height (µm)		**Valley height (µm)**		**Peak-peak distance (µm)**	
Vc	f	Experiments	FEM	Experiments	FEM	Experiments	FEM
40	0.2	-3.4%	8.4%	-20.0%	21.2%	25.4%	74.5%
50	0.2	-13.1%	8.8%	-27.2%	11.4%	-8.4%	33.3%
40	0.3	-8.3%	2.0%	-32.0%	-9.4%	30.7%	21.0%
50	0.3	-9.8%	4.9%	-21.8%	-1.7%	1.4%	19.8%

Table 5: Percentage difference in the median values of chip geometry between cryogenic and dry machining

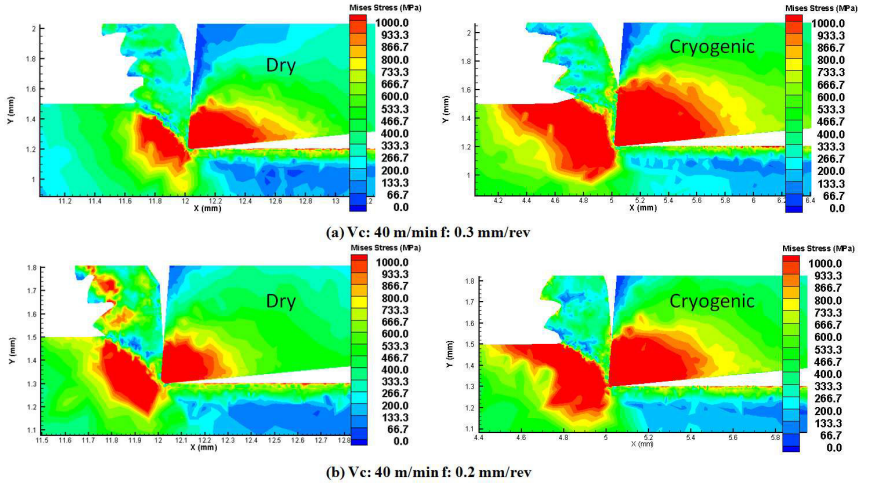

(a) Vc: 40 m/min f: 0.3 mm/rev

(b) Vc: 40 m/min f: 0.2 mm/rev

Figure 11: Stress distribution in dry and cryogenic cutting

5 Conclusions

In this study, finite element modeling is used to simulate 2D orthogonal cutting of Ti – 6Al – 4V titanium alloy, in order to analyze the effect of the two different cooling methods on serrated chip formation and cutting and thrust forces. Sensitivity analyses were performed on the jet radius and heat

convection coefficient to reach to the appropriate condition to simulate cryogenic cooling. The simulation predictions were compared with the experimental findings in order to validate the commercial simulation software and an acceptable prediction of cryogenic machining was achievable. Different cutting conditions were employed to obtain the least possible error between simulated and experimental values for cutting forces and chip formation. The finite element model was calibrated with dry machining experimental results to get the best possible FEM setting and then used for the cryogenic machining. The material model was used from software database and the coefficient of friction was held at a constant value for dry (0.55) and cryogenic (0.62) machining respectively, due to experimental findings. The predicted chip morphology is in good agreement with experimental results in terms of peak height, valley height and peak-peak distances for both dry and cryogenic cutting. In addition, acceptable results were obtained for cutting and thrust force prediction.

The comparison of dry and cryogenic simulations allows concluding that:

- The cutting forces and the coefficient of friction mildly increase with cryogenic turning.
- The level of stress obviously increases with cryogenic, in correlation with the force increase, but the location of maximum stress distributed in larger area in comparison with dry cutting.
- The chip segmentation frequency and the chip thickness in terms of peak height and valley height reduce with cryogenic machining.
- These considerations can be a good starting point to achieve a deeper knowledge on the chip formation in both dry and cryogenic cutting.

6 References

Ali, M., Balasubramanian, R., Mohamed, B. and Khidhir, B. (2011). Effects of Coolants on Improving Machining Parameters while Mach-Inability Titanium Alloy (Ti-6Al-4V): A Review. *AMM*, 110-116, pp.1657-1666.

Ali, M., Khidhir, B., Ansari, M. and Mohamed, B. (2013). FEM to predict the effect of feed rate on surface roughness with cutting force during face milling of titanium alloy. *HBRC Journal*, 9(3), pp.263-269.

Arrazola, P. and Özel, T. (2010). Investigations on the effects of friction modeling in finite element simulation of machining. *International Journal of Mechanical Sciences*, 52(1), pp.31-42.

Arrazola, P., Özel, T., Umbrello, D., Davies, M. and Jawahir, I. (2013). Recent advances in modelling of metal machining processes. *CIRP Annals - Manufacturing Technology*, 62(2), pp.695-718.

Bermingham, M., Kirsch, J., Sun, S., Palanisamy, S. and Dargusch, M. (2011). New observations on tool life, cutting forces and chip morphology in cryogenic machining Ti-6Al-4V. *International Journal of Machine Tools and Manufacture*, 51(6), pp.500-511.

Bil, H., Kılıç, S. and Tekkaya, A. (2004). A comparison of orthogonal cutting data from experiments with three different finite element models. *International Journal of Machine Tools and Manufacture*, 44(9), pp.933-944.

Byrne, G., Dornfeld, D. and Denkena, B. (2003). Advancing Cutting Technology. *CIRP Annals - Manufacturing Technology*, 52(2), pp.483-507.

Calamaz, M., Coupard, D. and Girot, F. (2008). A new material model for 2D numerical simulation of serrated chip formation when machining titanium alloy Ti–6Al–4V. *International Journal of Machine Tools and Manufacture*, 48(3-4), pp.275-288.

Chiappini, E., Tirelli, S., Albertelli, P., Strano, M. and Monno, M. (2014). On the mechanics of chip formation in Ti–6Al–4V turning with spindle speed variation. *International Journal of Machine Tools and Manufacture*, 77, pp.16-26.

Corduan, N., Himbart, T., Poulachon, G., Dessoly, M., Lambertin, M., Vigneau, J. and Payoux, B. (2003). Wear Mechanisms of New Tool Materials for Ti-6AI-4V High Performance Machining. *CIRP Annals - Manufacturing Technology*, 52(1), pp.73-76.

Ezugwu, E. and Wang, Z. (1997). Titanium alloys and their machinability—a review. *Journal of Materials Processing Technology*, 68(3), pp.262-274.

Hong, S. and Ding, Y. (2001). Cooling approaches and cutting temperatures in cryogenic machining of Ti-6Al-4V. *International Journal of Machine Tools and Manufacture*, 41(10), pp.1417-1437.

Hong, S., Ding, Y. and Jeong, W. (2001). Friction and cutting forces in cryogenic machining of Ti–6Al–4V. *International Journal of Machine Tools and Manufacture*, 41(15), pp.2271-2285.

Johnson, G. and Cook, W. (1983). A constitutive model and data for metals subjected to large strains, high strain-rates and high temperature. *The 7th Symposium on Ballistic*, pp.541–547.

Khan, A. and Ahmed, M. (2008). Improving tool life using cryogenic cooling. *Journal of Materials Processing Technology*, 196(1-3), pp.149-154.

Li, R. and Shih, A. (2005). Finite element modeling of 3D turning of titanium. *Int J Adv Manuf Technol*, 29(3-4), pp.253-261.

Ma, J., Andrus, P., Condoor, S. and Lei, S. (2014). Numerical Investigation of Tool Performance in Milling of Ti-6Al-4V Alloy. *Proceedings of NAMRI/SME*, 42.

Man, X., Ren, D., Usui, S., Johnson, C. and Marusich, T. (2012). Validation of Finite Element Cutting Force Prediction for End Milling. *Procedia CIRP*, 1, pp.663-668.

Narutaki, N., Murakoshi, A., Motonishi, S. and Takeyama, H. (1983). Study on Machining of Titanium Alloys. *CIRP Annals - Manufacturing Technology*, 32(1), pp.65-69.

Oxley, P. (1966). Introducing strain-rate dependent work material properties into the analysis of orthogonal Cutting. *CIRP Annals Manufacturing Technology*, 13, pp.127-138.

Pervaiz, S., Deiab, I., Rashid, A. and Nicolescu, C. (2014). Experimental and Numerical Investigation of Ti6Al4V Alloy machinability using TiAlN Coated Tools. *Proceedings of NAMRI/SME*, 42.

Pu, Z., Umbrello, D., Dillon, O. and Jawahir, I. (2014). Finite Element Simulation of Residual Stresses in Cryogenic Machining of AZ31B Mg Alloy. *Procedia CIRP*, 13, pp.282-287.

Pusavec, F., Courbon, C., Rech, J., Kopac, J. and Jawahir, I. (2014). An Investigation of the Effect of Nitrogen Phase on Cryogenic Machining Performance and a Case Study on Machining of Inconel 718 Alloy. *ASME Proceedings*, 2.

Strano, M., Albertelli, P., Chiappini, E. and Tirelli, S. (2013). Experimental Evaluation of Innovative Tools for Ti-6Al-4V Turning. *KEM*, 554-557, pp.1941-1952.

Sun, S., Brandt, M. and Dargusch, M. (2010). Thermally enhanced machining of hard-to-machine materials—A review. *International Journal of Machine Tools and Manufacture*, 50(8), pp.663-680.

Sun, S., Harris, J. and Brandt, M. (2008). Parametric Investigation of Laser-Assisted Machining of Commercially Pure Titanium. *Advanced Engineering Materials*, 10(6), pp.565-572.

Venugopal, K., Paul, S. and Chattopadhyay, A. (2007). Growth of tool wear in turning of Ti-6Al-4V alloy under cryogenic cooling. *Wear*, 262(9-10), pp.1071-1078.

Yildiz, Y. and Nalbant, M. (2008). A review of cryogenic cooling in machining processes. *International Journal of Machine Tools and Manufacture*, 48(9), pp.947-964.

Zhao, Z. and Hong, S. (1992). Cooling strategies for cryogenic machining from a materials viewpoint. *Journal of Materials Engineering and Performance*, 1(5), pp.669-678.

Özel, T. (2006). The influence of friction models on finite element simulations of machining. *International Journal of Machine Tools and Manufacture*, 46(5), pp.518-530.

Özel, T., Sima, M., Srivastava, A. and Kaftanoglu, B. (2010). Investigations on the effects of multi-layered coated inserts in machining Ti–6Al–4V alloy with experiments and finite element simulations. *CIRP Annals - Manufacturing Technology*, 59(1), pp.77-82.